Cancer Letters 452 (2019) 178–190

Contents lists available at ScienceDirect

Cancer Letters

journal homepage: www.elsevier.com/locate/canlet

Original Articles

Melanoma cell adhesion molecule is the driving force behind the dissemination of melanoma upon S100A8/A9 binding in the original skin lesion

Youyi Chen[a,g], I Wayan Sumardika[a,n], Nahoko Tomonobu[a], I Made Winarsa Ruma[a,n], Rie Kinoshita[a], Eisaku Kondo[b], Yusuke Inoue[c], Hiroki Sato[d], Akira Yamauchi[e], Hitoshi Murata[a], Ken-ichi Yamamoto[a], Shuta Tomida[f], Kazuhiko Shien[d], Hiromasa Yamamoto[d], Junichi Soh[d], Ming Liu[g], Junichiro Futami[h], Kaori Sasai[i], Hiroshi Katayama[i], Miyoko Kubo[a], Endy Widya Putranto[j], Toshihiko Hibino[k,1], Bei Sun[l], Masahiro Nishibori[m], Shinichi Toyooka[d], Masakiyo Sakaguchi[a,*]

[a] Department of Cell Biology, Okayama University Graduate School of Medicine, Dentistry and Pharmaceutical Sciences, 2-5-1 Shikata-cho, Kita-ku, Okayama-shi, Okayama, 700-8558, Japan
[b] Division of Molecular and Cellular Pathology, Niigata University Graduate School of Medicine and Dental Sciences, 757, Ichiban-cho, Asahimachidori, Chuo-ku, Niigata-shi, Niigata, 951-8510, Japan
[c] Faculty of Science and Technology, Division of Molecular Science, Gunma University, 1-5-1 Tenjin-cho, Kiryu-shi, Gunma, 376-8515, Japan
[d] Department of Thoracic, Breast and Endocrinological Surgery, Okayama University Graduate School of Medicine, Dentistry and Pharmaceutical Sciences, 2-5-1 Shikata-cho, Kita-ku, Okayama-shi, Okayama, 700-8558, Japan
[e] Department of Biochemistry, Kawasaki Medical School, 577 Matsushima, Kurashiki-shi, Okayama, 701-0192, Japan
[f] Department of Biobank, Okayama University Graduate School of Medicine, Dentistry and Pharmaceutical Sciences, 2-5-1 Shikata-cho, Kita-ku, Okayama, 700-8558, Japan
[g] Department of General Surgery & Bio-Bank of General Surgery, The Fourth Affiliated Hospital of Harbin Medical University, Harbin, 150001, China
[h] Department of Medical and Bioengineering Science, Okayama University Graduate School of Natural Science and Technology, 3-1-1, Tsushima-Naka, Kita-ku, Okayama, 700-8530, Japan
[i] Department of Molecular Oncology, Okayama University Graduate School of Medicine, Dentistry and Pharmaceutical Sciences, 2-5-1 Shikata-cho, Kita-ku, Okayama-shi, Okayama, 700-8558, Japan
[j] Department of Pediatrics, Dr. Sardjito Hospital/Faculty of Medicine, Universitas Gadjah Mada, Yogyakarta, 55281, Indonesia
[k] Department of Dermatology, Tokyo Medical University, 6-7-1 Nishi-Shinjuku, Shinjuku-ku, Tokyo, 160-0023, Japan
[l] Department of Pancreatic and Biliary Surgery, The First Affiliated Hospital of Harbin Medical University, Harbin, Heilongjiang, China
[m] Department of Pharmacology, Okayama University Graduate School of Medicine, Dentistry and Pharmaceutical Sciences, 2-5-1 Shikata-cho, Kita-ku, Okayama-shi, Okayama, 700-8558, Japan
[n] Faculty of Medicine, Udayana University, Denpasar, 80232, Bali, Indonesia

ARTICLE INFO

Keywords:
S100 protein
Metastasis
Inflammation
Seed and soil hypothesis
Matrix metalloproteinase

ABSTRACT

Since metastasis accounts for the majority of cancer-associated deaths, studies on the mechanisms of metastasis are needed to establish innovative strategies for cancer treatment. We previously reported that melanoma cell adhesion molecule (MCAM) functions as a critical receptor for S100A8/A9, and binding of S100A8/A9 to MCAM results in the migration of melanoma cells to lung tissue. However, the critical role of MCAM in the original melanoma skin lesion is still not clear. In this study, we aimed to determine the importance of the S100A8/A9-MCAM axis in melanoma dissemination in a skin lesion as a critical early step for metastasis. Mechanistic studies revealed the downstream signaling of MCAM that signaled the induction of metastasis. S100A8/A9-MCAM binding activates mitogen-activated protein kinase kinase kinase 8 (MAP3K8), also termed TPL2, leading to strong activation of the transcription factor ETV4 and subsequent induction of matrix metalloproteinase-25 (MMP25), and finally to induction of melanoma lung tropic metastasis. Collectively, our results demonstrate a crucial role of the S100A8/A9-MCAM signaling axis in metastatic onset of melanoma cells and indicate that

Abbreviations: ETS, E26 transformation specific; ETV4, ETS translocation variant 4; MCAM, melanoma cell adhesion molecule; MMP25, matrix metalloproteinase-25; PEA3, polyoma enhancer activator 3; TPL2, tumor progression locus 2

* Corresponding author.
E-mail address: masa-s@md.okayama-u.ac.jp (M. Sakaguchi).

[1] Toshihiko Hibino passed away on June 1, 2016.

https://doi.org/10.1016/j.canlet.2019.03.023
Received 17 November 2018; Received in revised form 7 March 2019; Accepted 9 March 2019

strategies targeting the identified pathway may be useful for the establishment of innovative anti-cancer therapies.

1. Introduction

Melanoma is a life-threatening disease due to its rapid and aggressive dissemination to remote areas (metastasis), which can cause serious organ dysfunctions [1,2]. A better understanding of the systematic induction of metastasis at the molecular level is needed to establish an effective strategy for metastatic cancer therapy.

For some time now, cancer researchers have noticed that certain organs appear to be favored for metastasis of particular cancers. In 1889, Stephen Paget proposed the "seed and soil" hypothesis to explain the interesting relationship between cancer cells and their pre-metastatic organ of preference [3]. However, there is still insufficient molecular-level evidence to validate this theory.

Much progress has recently been made in the understanding of organ-specific metastasis. Hiratsuka et al. showed that S100A8/A9, a heterodimer complex of S100A8 and S100A9 proteins, functions as a strong soil signal in the pre-metastatic lung; S100A8/A9 attracts seed melanoma cells to the area in which it is produced through a soil signal sensor, toll-like receptor 4 (TLR4), that is expressed in the cancer region [4]. Like TLR4, the receptor for advanced glycation endproducts (RAGE) also acts as an S100A8/A9 receptor, and binding of S100A8/A9 to RAGE leads to the migration of melanoma cells to lung tissue [5]. We have recently reported two other receptors that are important for melanoma organ-specific metastasis: extracellular matrix metalloproteinase inducer (EMMPRIN) and melanoma cell adhesion molecule (MCAM) [6–8]. Interestingly, we found that EMMPRIN favors S100A9 and that their binding resulted in the migration of melanoma cells into the bloodstream and subsequent accumulation in artificially S100A9-enriched skin tissue in a mouse model [6]. MCAM, which responds to S100A8/A9, induces lung-specific metastasis of melanoma cells in which it is expressed [8]. These receptors may therefore coordinately function in melanoma cells to produce the driving force leading to S100A8/A9-mediated organ-specific metastasis. It has been shown that EMMPRIN triggers its own downstream signal onset, which links to NF-κB activation through the TRAF2 adaptor [7]. However, insufficient progress has been made in elucidation of the MCAM downstream signals.

The aim of this study was to determine the signal pathway triggered by MCAM activation upon S100A8/A9 binding. We revealed for the first time that ETS translocation variant 4 (*ETV4*), also known as polyoma enhancer activator 3 (PEA3), which exists downstream of MCAM, is a key transcription factor (TFs) for inducing melanoma metastasis through significant induction of matrix metalloproteinase-25 (MMP25). We also found that mitogen-activated protein kinase kinase kinase 8 (MAP3K8), termed TPL2, which binds to MCAM, plays a key role in the activation of ETV4. Finally, our findings revealed that the novel pathway triggered by MCAM-S100A8/A9 binding enhances dissemination of melanoma in the original skin lesion and subsequent lung metastasis. These results should contribute to our understanding of the molecular mechanisms underlying the complex regulatory maze of cancer metastasis.

2. Materials and methods

2.1. Cell lines and reagents

The following cell lines were used in this study: normal human melanocytes (NMC; KURABO Lifeline Cell Technology, Osaka, Japan), normal human keratinocytes (NHK; KURABO Lifeline Cell Technology), HEK293T (a human embryonic kidney cell line stably expressing the SV40 large T antigen; RIKEN BioResource Center, Tsukuba, Japan), two human melanoma cell lines established from the same patient—*i.e.*, WM-115 (derived from the primary tumor; ATCC, Rockville, MD) and WM-266-4 (derived from a metastatic site; ATCC)—and mouse melanoma cell line B16-BL6, a highly invasive variant of the mouse melanoma B16 cell line (a kind gift from Dr. Isaiah J. Fidler, M.D., Anderson Cancer Center, Houston, TX).

NMC was maintained in DermaLife® Basal Medium (KURABO Lifeline Cell Technology) supplemented with a DermaLife® M LifeFactors Kit (KURABO Lifeline Cell Technology). NHK was maintained in HuMedia-KG (KURABO Lifeline Cell Technology) supplemented with 10 μg/ml insulin, 0.1 ng/ml hEGF, 0.67 μg/ml hydrocortisone hemisuccinate and bovine pituitary extract (BPE) (KURABO Lifeline Cell Technology). HEK293T, WM-115 and WM-266-4 were cultivated in D/F medium (Thermo Fisher Scientific, Waltham, MA) supplemented with 10% FBS (Intergen, Purchase, NY). U0126, a selective inhibitor of ERK1/2, was purchased from Sigma-Aldrich (St. Louis, MO). All cultures were regularly checked for mycoplasma by using both a mycoplasma detection kit (Thermo Fisher Scientific) and Hoechst 33342 staining. Authentication of WM-115, WM-266-4 and B16-BL6 was verified by short tandem repeat DNA profiling.

2.2. Preparation of recombinant S100A8/A9

Human S100A8/A9 recombinant protein was prepared using the FreeStyle 293 Expression System (Thermo Fisher Scientific) as previously reported [8]. Briefly, after transfection of the 293-F cells (1×10^6 cells) with 150 μg of an expression plasmid carrying both the human S100A8 and S100A9 genes using 293-Fectin-transfection reagent (Thermo Fisher Scientific), the cells were cultivated in a 500-mL flask filled with 150 ml of medium using an orbital shaker (125 rpm) at 37 °C in the presence of 8% CO_2 for 4 days. The culture medium, which included the S100A8/A9 secreted from the cultured cells, was collected and concentrated by an Amicon Ultra centrifugal filter unit (Merck Millipore, Billerica, MA). Subsequently, S100A8/A9 protein in the concentrated medium was captured by Talon® Metal affinity resin (Takara Bio, Shiga, Japan) and eluted with 150 mM imidazole. The solution including S100A8/A9 recombinant protein was exchanged for PBS using a Sephadex G25 M column chromatograph (GE Healthcare, Piscataway, NJ) and sterilized with 0.22-μm Millex-GV syringe filters (Merck Millipore).

2.3. Plasmid constructs

To induce efficient expression of the transgenes in a temporal manner, we inserted the cDNAs of interest into pIDT-SMART (C-TSC) vector [9]. The prepared cDNAs were as follows: human cDNAs encoding MCAM, MCAM dn (deletion of cytoplasmic tail: 584–646 aa), ETS family genes (ETV1, ETV4, ETV5, ELK, EHF, ERG, ELF, FEV and SPDEF), ETV4 dn (deletion of C-terminal DNA binding domain: 342–484 aa), MAPK cascade upstream kinases (NAK, NIK, TAK1, DLK, TPL2, ASK1, SPRK, MLK1, MEKK3, LZK, MLK4, ARAF, BRAF, CRAF, MOS and MKK5) and a kinase dead type of TPL2 [TPL2 mut (KD); 167K replaced by M]. MCAM and MCAM dn were designed for expression as C-terminal 3xHA-6His-tagged forms. ETS family genes, ETV4 dn, MAPK cascade upstream kinases and TPL2 mut (KD) were designed for expression as C-terminal Myc-6His-tagged forms. Cells were transiently transfected with the plasmid vectors using FuGENE-HD (Promega, Madison, WI).

To obtain foreign gene-overexpressing clones that show significantly high expression levels of the transduced genes in an efficient and stable manner, we improved the pIDT-SMART (C-TSC) to a stable expression version, resulting in two types of improved plasmids, named pSAKA-1B [7] and pSAKA-4B [10]. The expression vector pSAKA-1B can be used for expression in Chinese hamster ovary (CHO) cells at a

very high level, while pSAKA-4B is adapted to express significantly high levels of the target genes in a wide range of mammalian cell lines from different species in a constant manner. We therefore used pSAKA-4B to establish B16-BL6-based clones in this study. MCAM (wt)-3xHA-6His and ETV4 (wt and dn)-3xMyc-6His were inserted into pSAKA-4B. Human MMP25, which was designed to express either of the N-terminal 3xHA-tagged forms (see Supplementary Fig. S7A), was also inserted into the same vector. A series of clones (see Supplementary Figs. S3 and S4, S7B-S7I) were established by a convenient electroporation gene delivery method and subsequent selection with puromycin at 20 μg/ml.

2.4. Quantitative real-time PCR analysis

The prepared mRNAs (500 ng) from cultured cells (1×10^6 cells) were reversed to cDNAs by SuperScriptTM II (Thermo Fisher Scientific). The cDNA solutions were diluted 1:10 in MilliQ water and used for the next PCR reaction. Real-time RT-PCR was performed using a LightCycler rapid thermal cycler system (ABI 7900HT; Applied Biosystems, Foster City, CA) with LightCycler 480 SYBR Green I Master Mix (Roche Diagnostics, Indianapolis, IN). The forward and reverse primer pairs used (5′ to 3′) are listed in Table S4. TBP expression was used as a reliable calibration control.

2.5. SiRNA and decoy DNA

Human MCAM siRNAs (#1 ID No. s8571, #2 ID No. s8572), mouse Mmp25 siRNAs (#1 ID No. s109154, #2 ID No. s109155, #2 ID No. s109156) and control siRNA (Silencer Negative control siRNA) were purchased from Thermo Fisher Scientific. Decoy DNAs for four transcription factors—ETS, GATA, NFI and PPAR—were prepared by hybridizing primer pairs corresponding to each TF. The primer sequences are shown in Supplementary Table S2 siRNAs (50 nM) and decoy DNAs (1 μM) were transfected into cells (3×10^5 cells) using Lipofectamin RNAiMAX reagent (Thermo Fisher Scientific).

2.6. Co-immunoprecipitation and western blotting

Co-immunoprecipitation and Western blotting are described in the Supplementary Materials and Methods.

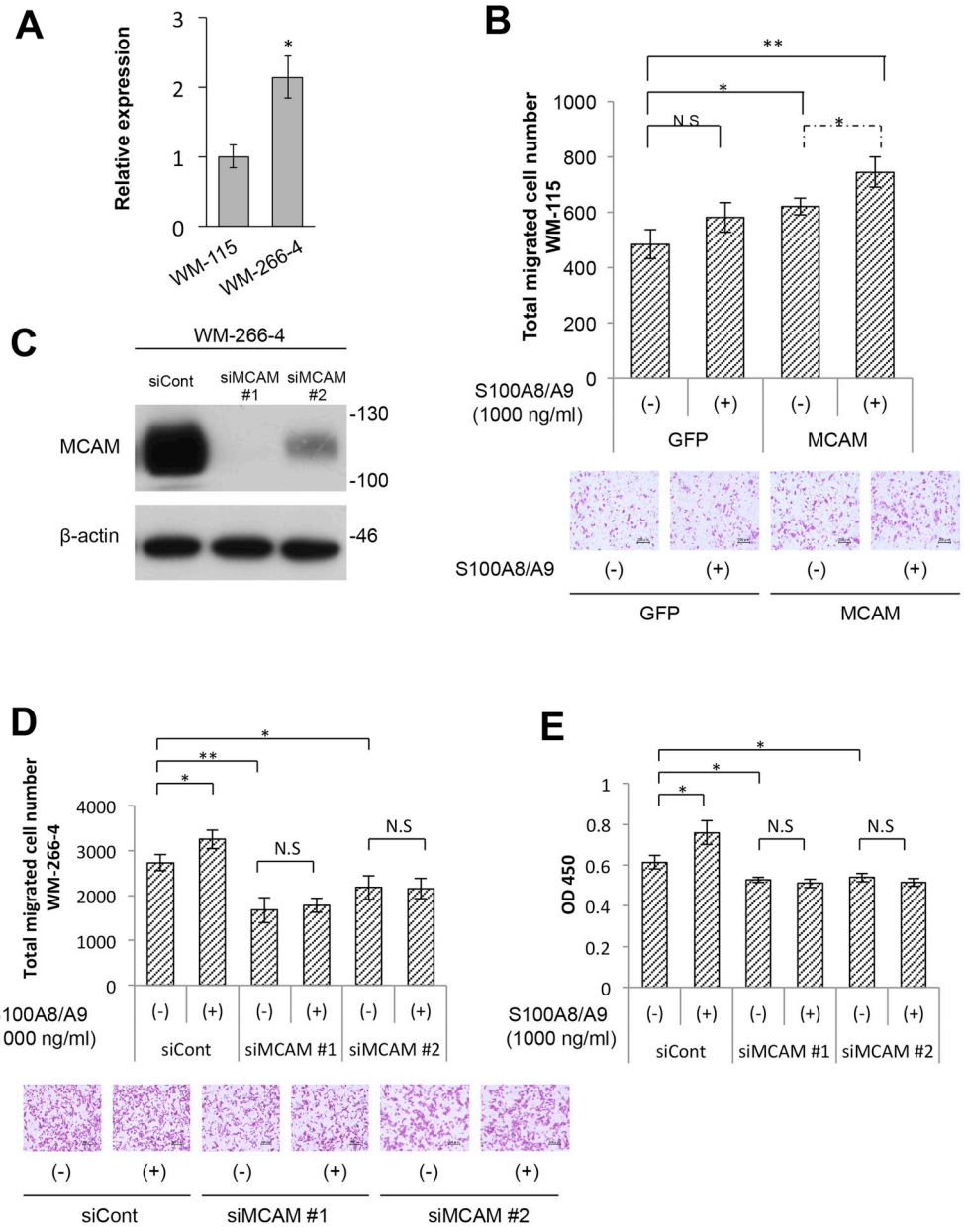

Fig. 1. MCAM stimulates cellular migration and growth in response to S100A8/A9 in melanoma cells. A, Quantitative real-time PCR analysis was carried out in WM-115 and WM-266-4 cells for the *MCAM* gene. The relative expression level in each sample after calibration with the TBP value is shown. B, Migration of WM-115 cells transfected with the indicated gene (GFP as a control or MCAM) was assessed by the Boyden chamber method. The transfected cells were placed in the top chamber, and purified recombinant S100A8/A9 (1000 ng/ml) was added (+) or not added (−) to the bottom well. Quantified results are shown in the upper panel and representative images of migrating cells are shown in the bottom panel. C, WM-266-4 cells were transfected with either siMCAM or a negative control scrambled siCont, and cellular MCAM protein in the treated cells was detected by WB. D, siRNA-treated WM-266-4 cells were assessed for their migration abilities in response to extracellular S100A8/A9 (1000 ng/ml) by the same method described in (B). E, siRNA-treated WM-266-4 cells were also evaluated for their growth conditions by MTS assay in the presence (+) or absence (−) of S100A8/A9 (1000 ng/ml) in the media. Data are means ± SD; N.S: not significant; *P < 0.05, **P < 0.01 and ***P < 0.001.

2.7. Immunocytochemistry and immunohistochemistry

Immunocytochemistry and immunohistochemistry are described in the Supplementary Materials and Methods.

2.8. Protein/DNA array and electrophoretic mobility shift assay (EMSA)

Screening of activated TFs through MCAM overexpression in HEK293T cells (1×10^6 cells) was performed by using a protein/DNA array I (Thermo Fisher Scientific) according to the manufacturer's instructions.

Nuclear extracts from WM-266-4 cells (1×10^6 cells) were prepared according to the manufacturer's instructions using NE-PER Nuclear and Cytoplasmic Extraction Reagents (Thermo Fisher Scientific), and EMSA was performed using a LightShift Chemiluminescent EMSA kit (Thermo Fisher Scientific). A 5′-biotin-labeled double-stranded probe (forward: 5′-agtacCGGAAGTaca-3′; reverse: 3′-tgtACTTCCGgtact-5′) was purchased from Sigma-Aldrich. Rabbit anti-human PEA3/ETV4 antibody (Novus, Littleton, CO) was used for super shift analysis. After the reactions, all samples were fractionated by 7% PAGE and blotted onto a Biodyne B nylon membrane (Pall, Tokyo).

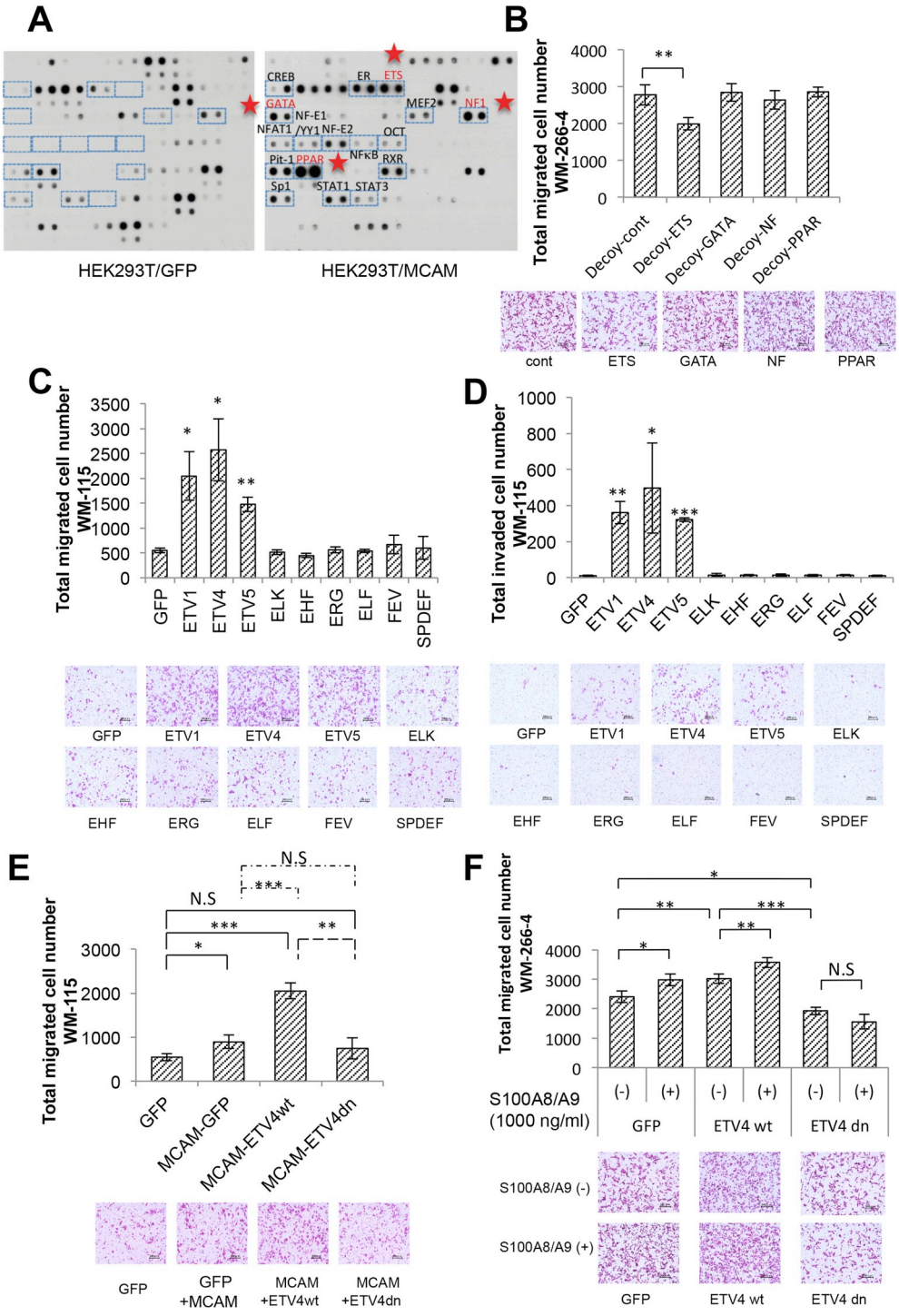

Fig. 2. Identification of ETV4, which plays a pivotal role in S100A8/A9-MCAM-mediated upregulation of cellular motility. A, A protein/DNA array was used to detect activated transcription factors by MCAM overexpression in HEK293T cells. B, WM-266-4 cells were transfected with the indicated decoy DNA fragments (0.1 μM) and then subjected to the Boyden chamber-based migration assay. C, D, WM-115 cells were temporally overexpressed with the indicated gene expression plasmids and then plated on the top surface of non-sealed inserts (C) or Matrigel-sealed inserts (D). The migrating cells that passed through the filter membranes in the top inserts were evaluated. E, WM-115 cells were co-transfected with MCAM + GFP, MCAM + ETV4 wt or MCAM + ETV4 dn, and the transfectants were assessed for their migration abilities. F, WM-266-4 cells with overexpression of the indicated genes were assessed for their migration abilities in the presence (+) or absence (−) of S100A8/A9 (1000 ng/ml) in the bottom media. Data are means ± SD; N.S: not significant; *P < 0.05, **P < 0.01 and ***P < 0.001.

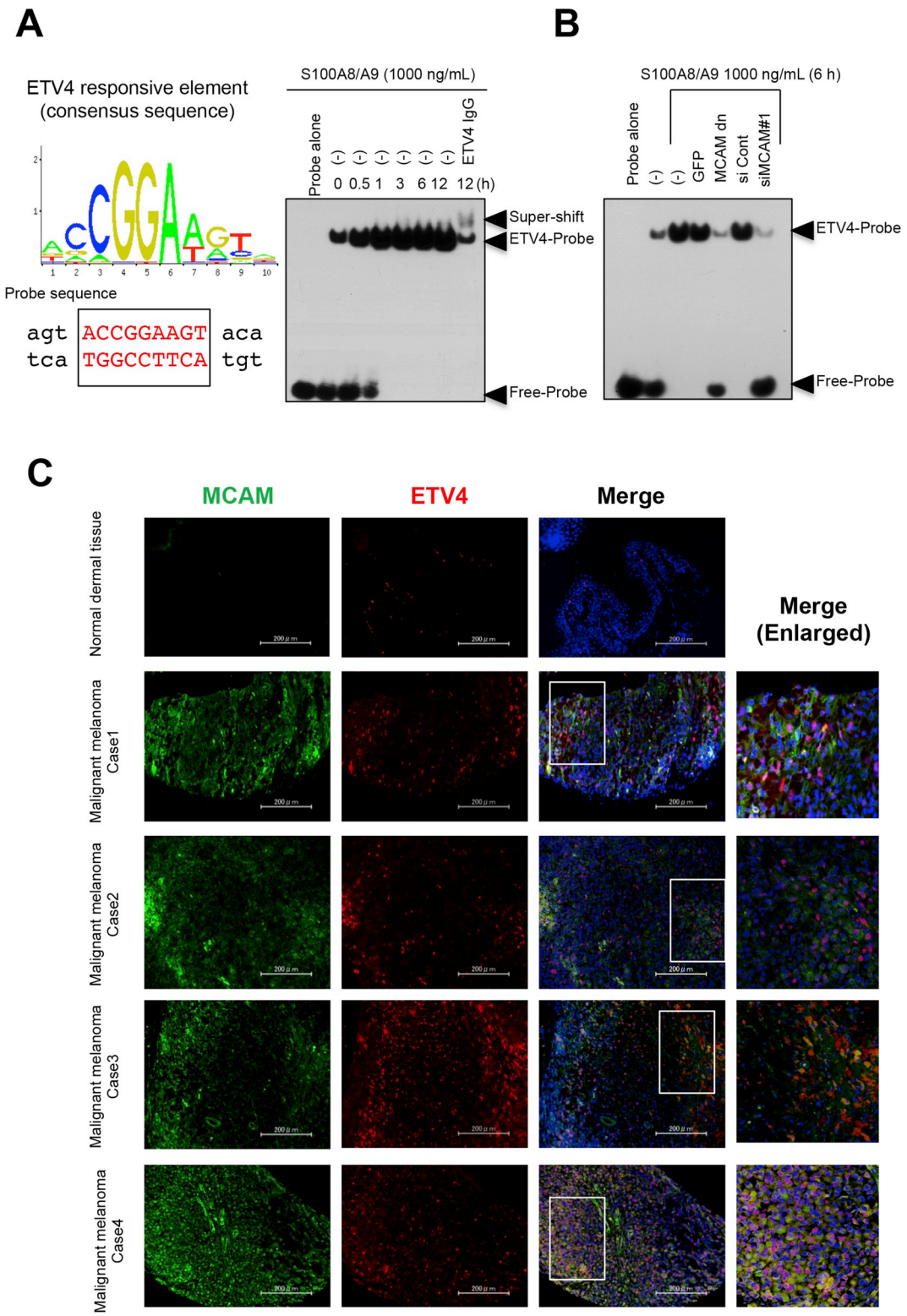

Fig. 3. An electrophoretic mobility shift assay (EMSA) was performed in WM-266-4 nuclear extracts with a biotin-conjugated double stranded oligonucleotide probe that is specific for binding with ETS family proteins. A, A consensus ETV4-responsive sequence was used as a probe (left panel). The sequence was designed on the basis of a publicly available database (JASPAR matrix model:http://jaspar.genereg.net/cgi-bin/jaspar_db.pl?rm=browse&db=core&tax_group=vertebrates). WM-266-4 cells were treated with S100A8/A9 (1000 ng/ml) at regular time intervals. ETV4-specific binding was confirmed by the appearance of a super-shift band using ETV4 IgG (right panel). B, ETV4 activation was evaluated after transfection of WM-266-4 cells with either MCAM DN plasmid or MCAM siRNA (siMCAM #1) and subsequent treatment of the transfectants with S100A8/A9 (1000 ng/ml) for six hours. C, Expression and localization of MCAM and ETV4 in clinical melanoma samples. Paraffin-embedded human melanoma sections were co-stained with MCAM antibody (green) and ETV4 antibody (red). Representative images of MCAM and ETV4 staining (Scale, 200 μM). . (For interpretation of the references to color in this figure legend, the reader is referred to the Web version of this article.)

2.9. Luciferase-based reporter gene assay

The human MMP25 promoter (3237 bp with SacI and HindIII sites from the translation start site) was cloned into the luciferase reporter vector pGL4.11 (Promega), yielding pGL4.11-pMMP25-Luc. Either the pGL4.11-pMMP25-Luc or pGL4.74 vector encoding *Renilla* luciferase regulated under the HSV-TK promoter as an internal control (Promega) was transfected into HEK293T cells (2×10^4 cells) using the transfection reagent polyethyleneimine Max (Polyscience, Warrington, PA). For co-transfection, pIDT-SMART (C-TSC)-ETV4-wt and –ETV4-dn were used for the MMP25 promoter. After 48 h, the transfected cells were washed with PBS and promoter activities were measured using the Dual-Luciferase Reporter Assay System (Promega).

2.10. Cell proliferation assay

Cells (5×10^3 cells/well) were seeded in 96-well plates. Cell proliferation was evaluated by using a Cell-Titer-Glo™ Luminescent Cell Viability assay kit (Promega) according to the manufacturer's instructions.

2.11. Migration and invasion assays

Migration and invasion assays were performed by the Boyden chamber method as described in the Supplementary Materials and Methods.

2.12. Animal experiments

Experimental protocols were approved by the Animal Experiment Committee of Okayama University (approval No. OKU-2014011). All mouse procedures and euthanasia, including cell transplantations, were done painlessly or under inhalation anaesthesia with isoflurane gas according to the strict guidelines of the Experimental Animal Committee of Okayama University. To examine tumor metastasis *in vivo*, B16-BL6-originated clones were used in animal experiments. The established clones (1×10^5 cells) were injected into the tail veins of immunocompetent Balb/c mice at the age of 6 weeks (Charles River Laboratories, Yokohama, Japan). Three weeks later, metastasized melanoma distributed throughout the lung was observed by LaTheta® X-ray computed tomography (CT-scan; Hitachi-Aloka Medical, Tokyo) and then the lung metastasis was assessed by counting the formed melanoma foci after sacrificing the tumor-bearing mice.

2.13. Statistical analysis

Data shown are the means ± SD calculated using at least three independent experiments. Significant differences between the mean values of each group were determined by Student's *t*-test.

3. Results

3.1. MCAM stimulates cellular migration and growth in response to S100A8/A9 in melanoma cells

To examine the role of MCAM in melanoma in response to S100A8/A9, we first used two human melanoma cell lines, WM-115 and WM-266-4, obtained from the same patient. The WM-115 cell line was from the primary tumor in the skin and the WM-266-4 cell line was established from a metastasized lymph node [11]. We found that the MCAM expression level was about two-fold higher in metastatic WM-266-4 cells than in non-metastatic WM-115 cells (Fig. 1A). When foreign MCAM was overexpressed in WM-115 cells, the migration ability in response to S100A8/A9 stimulation was upregulated (Fig. 1B). Intrinsic MCAM in WM-266-4 cells was downregulated by specific siRNAs (Fig. 1C) and its effect on cellular motility was evaluated. By this approach, we found that suppression of MCAM expression eliminates not only the innate power of migration but also its enhancement by S100A8/A9 stimulation (Fig. 1D). The S100A8/A9-mediated enhancement of growth was also diminished by the reduction of MCAM in WM-266-4 cells (Fig. 1E). These *in vitro* data (Fig. 1) together with previous imaging of S100A8/A9 in a melanoma skin lesion suggest that extracellular S100A8/A9 from keratinocytes plays a critical role in melanoma progression, including growth and spread at the primary tumor site, through melanoma cell surface MCAM. In addition, melanoma progression might be greatly affected by the MCAM expression level.

3.2. Identification of ETV4, which plays a pivotal role in S100A8/A9-MCAM-mediated upregulation of cellular motility

We then tried to investigate the S100A8/A9 binding-activated, MCAM downstream signal that induces the metastatic signaling cascade in melanoma. The first screening of TFs provided several candidates that were activated by MCAM overexpression in HEK293T cells (Fig. 2A and Supplementary Table S1). With respect to the several parameters examined—namely, higher induction, novelty, and links to cancer progression—we identified four TFs that met all the criteria, ETS, GATA, NFI and PPAR, from which we attempted to select a single TF that was very highly associated with S100A8/A9-MCAM-mediated upregulation of cellular motility. By means of a second screening using DNA decoys (Supplementary Table S2), *i.e.*, synthetic short DNA *cis*-elements for TF binding, which compete with intranuclear DNA and reduce the function of TFs, we found that only the ETS DNA decoy attenuated the migration capacity of WM-266-4 cells (Fig. 2B). It has long been recognized that some ETS family members act as oncogenic proteins [12-15]. We therefore carried out expression profiling of ETS family members in melanoma cell lines (Supplementary Fig. S1). From our data, we selected ETS genes that were significantly more highly expressed in melanoma cells than in NMC across all or only some of the melanoma cell lines examined. The selected genes were ETV1, ETV4, ETV5, ELK, EHF, ERG, ELF, FEV and SPDEF. This led us to reexamine the cellular disseminative activity for the selected genes. Fig. 2 (C and D) shows that three genes, ETV1, ETV4 and ETV5, have the ability to significantly enhance both the migration and invasion of WM-115 cells even with no S100A8/A9 stimulation. To identify the gene that contributes most to melanoma progression, we constructed dominant negative (dn) forms of the gene with loss of DNA binding capacity. After transfection of the constructs (ETV1 dn, ETV4 dn and ETV5 dn expression vectors), we found that the greatest reduction in innate migration ability was for ETV4 dn-overexpressed WM-266-4 cells. In accordance with this, S100A8/A9 responsiveness was also diminished (Supplementary Fig. S2). These results indicated that ETV4 plays a crucial role in melanoma progression through the S100A8/A9-MCAM signaling axis, and they were further confirmed in a subsequent assay in which overexpression of the ETV4 wt remarkably enhanced MCAM-mediated migration, while ETV4 dn inhibited the function of MCAM in WM-115 cells (Fig. 2E). Furthermore, in WM-266-4 cells, ETV4 dn led to a marked reduction of both innate migration activity and the activity induced by S100A8/A9 (Fig. 2F).

We next examined whether activation of intrinsic ETV4 actually occurs in response to S100A8/A9 stimulation in WM-266-4 cells. As shown in Fig. 3A, we confirmed that the DNA binding activity of ETV4 was greatly increased in a time-dependent manner. In turn, the S100A8/A9-mediated activation of ETV4 was suppressed by either MCAM dn overexpression or MCAM siRNA transduction (Fig. 3B), indicating that ETV4 activation is largely regulated by the S100A8/A9-MCAM signaling axis in melanoma cells.

To confirm that MCAM-positive melanoma expresses ETV4 under physiological conditions, we compared the results of IHC staining for MCAM and ETV4 in clinical samples of skin malignant melanoma with those in normal skin tissue. Strong nuclear staining of ETV4 was partially observed in MCAM-positive melanoma in all cases examined

(Fig. 3C), suggesting the presence of a highly aggressive population (MCAM + ETV4 double-positive) throughout the entire melanoma mass.

3.3. TPL2 is a critical activator of ETV4 in the S100A8/A9-MCAM signaling cascade

Constitutively active mutation of the *BRAF* gene is a critical event in melanomagenesis and subsequent malignant progression that occurs in 50%–70% of all melanomas [16–18]. BRAF belongs to the mitogen-activated protein kinase kinase kinase (MAP3K) family. We therefore considered that MAP3Ks including BRAF might greatly contribute to the S100A8/A9-MCAM-ETV4 pathway we newly identified. To investigate this possibility, we examined the potential interactions between MCAM and MAPKs. Our candidate screening method for protein-protein interactions provided novel partners of MCAM for its downstream signaling, *i.e.*, four MAP3Ks (DLK, TPL2, ASK1 and MLK1) and one MAP2K (MKK5) (Fig. 4A). Among these, TPL2 alone possessed a high ability to induce upregulation of cellular motility in WM-115 cells (Fig. 4B). Moreover, TPL2 significantly enhanced ETV4-mediated migration, and this enhancement was not observed when ETV4 dn was overexpressed in WM-115 cells (Fig. 4C). To confirm the importance of TPL2, we constructed an established kinase-dead mutant of TPL2, TPL2 mut (KD), and assessed its effect on the migration of MCAM-highly-positive WM-266-4 cells. Although the TPL2 wt noticeably increased the innate activity of migration and S100A8/A9 stimulation further enhanced the activity, TPL2 mut (KD) showed almost the same level of migration activity as the control GFP with or without S100A8/A9

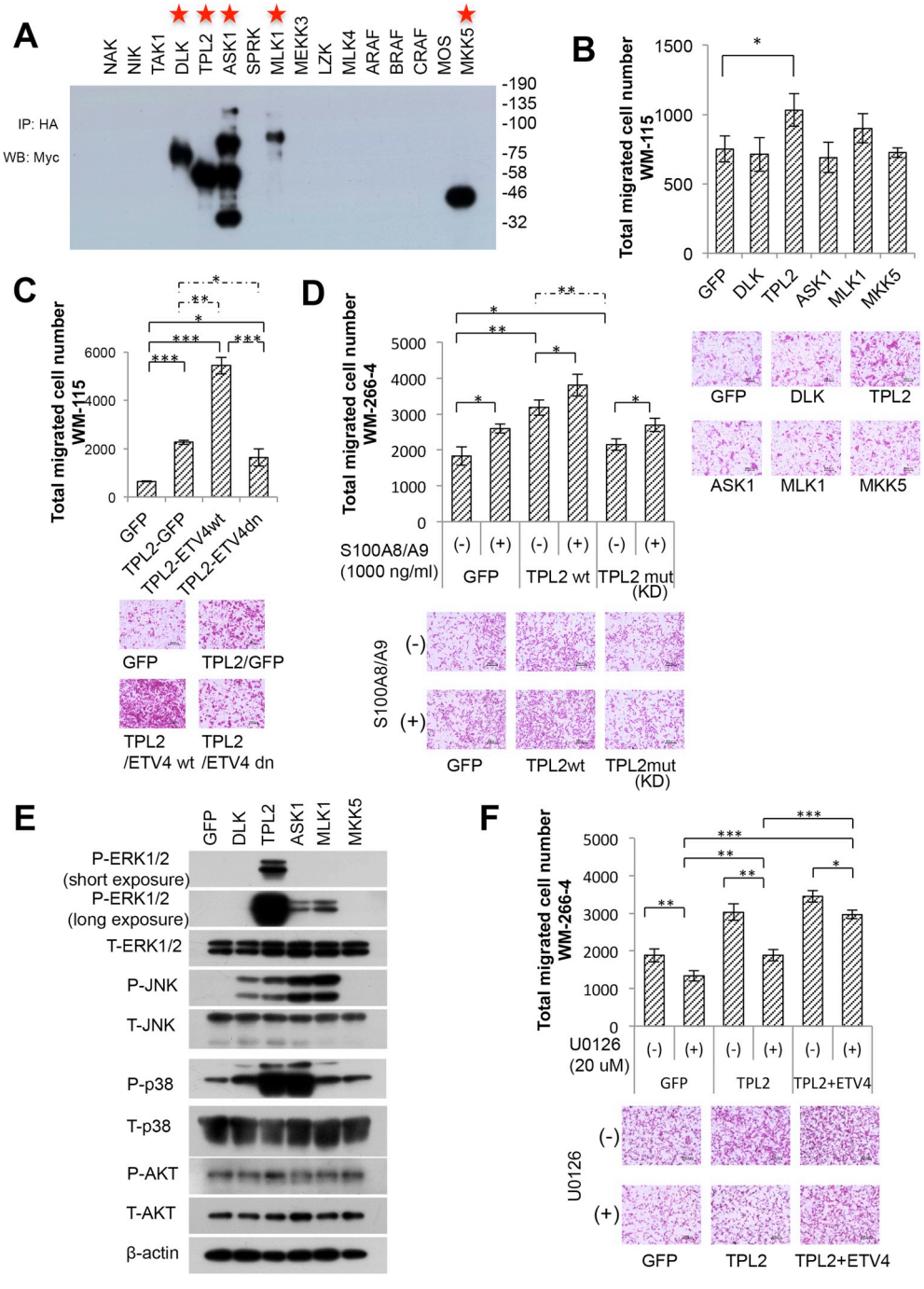

Fig. 4. TPL2 is a critical activator of ETV4 in the S100A8/A9-MCAM signaling cascade. A, HEK293T cells were co-transfected with HA-tagged MCAM and Myc-tagged upstream kinases: NAK (NF-κB-Activating Kinase: *TBK1*), NIK (NF-κB-Inducing Kinase: *MAP3K14*), TAK1 (TGF-β-Activated Kinase 1: *MAP3K7*), DLK (Dual Leucine Zipper-Bearing Kinase: *MAP3K12*), TPL2 (Tumor Progression Locus 2: *MAP3K8*), ASK1 (Apoptosis Signal-Regulating Kinase 1: *MAP3K5*), SPRK (Src-Homology 3 Domain-Containing Proline-Rich Kinase: *MAP3K11*), MLK1 (Mixed Lineage Kinase 1: *MAP3K9*), MEKK3 (MAPK/ERK Kinase Kinase 3: *MAP3K3*), LZK (Leucine Zipper-Bearing Kinase: *MAP3K13*), MLK4 (Mixed Lineage Kinase 4: *MAP3K21*), ARAF (A-Raf Proto-Oncogene, Serine/Threonine Kinase: *ARAF*), BRAF (B-Raf Proto-Oncogene, Serine/Threonine Kinase: *BRAF*), CRAF (C-Raf Proto-Oncogene, Serine/Threonine Kinase: *RAF1*), MOS (MOS Proto-Oncogene, Serine/Threonine Kinase: *MOS*), and MKK5 (MAP Kinase Kinase 5: *MAP2K5*). After immunoprecipitation of the expressed MCAM with HA antibody-conjugated beads, interacting kinases were detected by the Myc antibody. Asterisks show the candidates that interacted with MCAM. B, Five candidate kinases as indicated were transfected into WM-115 cells and their effects on migration were assessed. C, WM-115 cells were co-transfected with TPL2 + GFP, TPL2 + ETV4 wt or TPL2 + ETV4 dn, and the transfectants were assessed for their migration abilities. D, WM-266-4 cells with overexpression of GFP, TPL2 wt or a kinase dead type (K167 M) of TPL2 [TPL2 mut (KD)] were assessed for their migration abilities in the presence (+) or absence (−) of S100A8/A9 (1000 ng/ml) in the bottom media. E, WB analysis of the phosphorylation of effector kinases including ERK1/2, SAPK/JNK (JNK), p38, and AKT was carried out by using HEK293T cell extracts with transfection of GFP, DLK, TPL2, ASK1, MLK1 or MKK5. F, Migration evaluation was performed in WM-266-4 cells by the same method described in (D) except for the presence (+) or absence (−) of an ERK1/2 selective inhibitor, U0126 (20 μM), in the culture media. Data are means ± SD; N.S: not significant; *P < 0.05, **P < 0.01 and ***P < 0.001.

treatment (Fig. 4D). The slight responsiveness of S100A8/A9 in the case of TPL2 mut (KD) was probably due to endogenous TPL2 in WM-266-4 cells. It has been reported that ETV4 activation is positively regulated by ERK1/2 effector kinase [19–21], and we further investigated whether TPL2 can result in activation-linked phosphorylation of ERK1/2. As shown in Fig. 4E, we found that TPL2 significantly induced ERK1/2 phosphorylation. When we treated WM-266-4 cells with a selective ERK1/2 inhibitor, U0126, the TPL2-induced marked elevation of migration was reduced to the level in non-treated control GFP cells, and ETV4 overexpression effectively impaired the U0126-induced reduction of migration (Fig. 4F). Taken together, these results strongly suggest that TPL2 plays a crucial role in ETV4 activation through ERK1/2 phosphorylation in the region downstream of cell surface MCAM in response to extracellular S100A8/A9 stimulation, which eventually leads to acquisition of an advanced spreading phenotype in melanoma cells.

3.4. ETV4 activation through the S100A8/A9-MCAM axis is critical for melanoma growth and lung metastasis

To clarify the significance of the identified pathway in melanoma in *in vivo* metastasis processes, we established several stable transformants (control GFP, MCAM alone, ETV4 wt alone, ETV4 dn alone, MCAM + ETV4 wt, MCAM + ETV4 dn) from mouse melanoma B16-

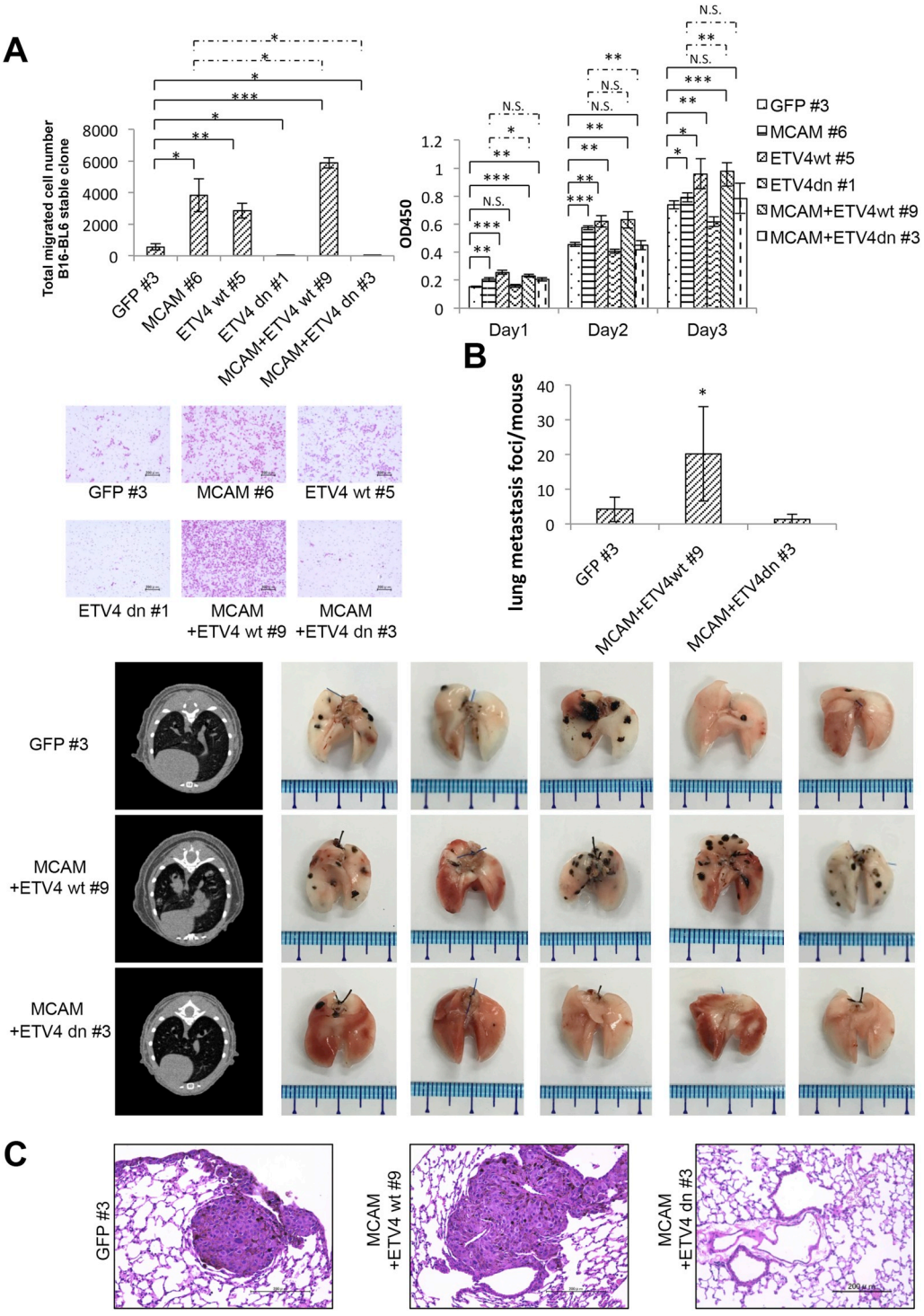

Fig. 5. ETV4 activation through the S100A8/A9-MCAM axis is critical for melanoma growth and lung metastasis. B16-BL6 cell-based stable transformants with stable overexpression of foreign genes, GFP alone as a control, MCAM alone, ETV4 wt alone, ETV4 dn alone, MCAM + ETV4 wt and MCAM + ETV4 dn were established (see Materials and Methods; Supplementary Figs. S3 and S4). A representative clone in each group was selected and examined for the growth and metastasis in both *in vitro* and *in vivo* experimental settings. A, Cellular migration (left) and growth (right) were assessed in the representative clones by the Boyden chamber method and MTS assay, respectively. B, Each representative clone (1×10^5 cells) was injected into mice through the tail vein. Three weeks later, lung metastatic nodules were quantified (top). The lung tumor nodules were observed macroscopically (bottom, CT scan images and resected whole lung pictures) and their sections were also observed by H&E staining (C). n = 5. Data are means ± SD; N.S: not significant; *P < 0.05, **P < 0.01 and ***P < 0.001.

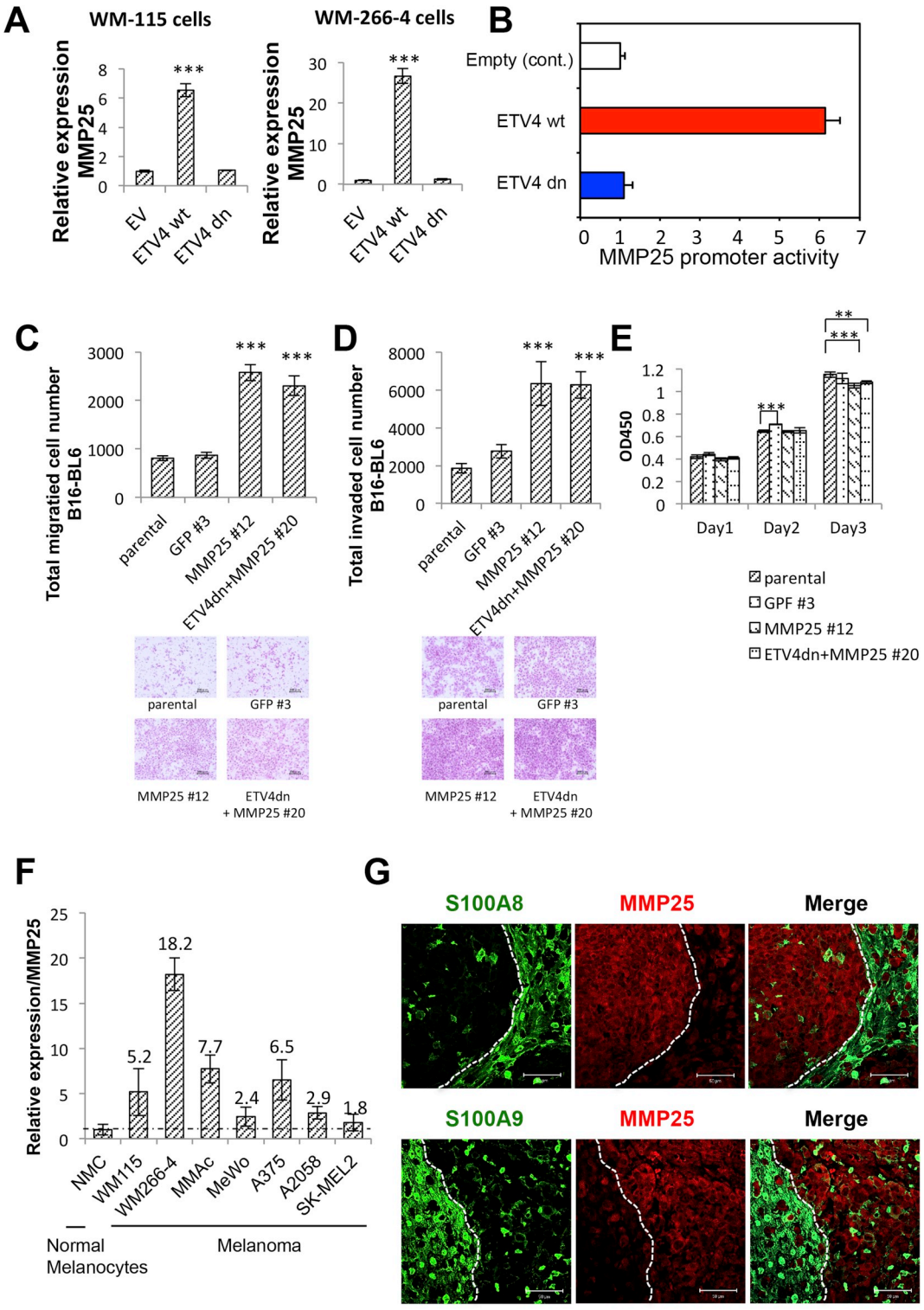

Fig. 6. MMP25, a key molecule for the regulation of melanoma motility and invasiveness, is strongly induced by ETV4 activation through the S100A8/A9-MCAM axis. A, Quantitative real-time PCR analysis was carried out in WM-115 (right) and WM-266-4 (left) for *MMP25* genes. Total RNAs were prepared from these genes with overexpression of an empty vector (EV), ETV4 wt or ETV4 dn. The relative expression level in each sample after calibration with the TBP value is shown. B, ETV4-mediated promoter activation of MMP25 was evaluated by the luciferase-based reporter gene assay. HEK293T cells were co-transfected with pGL4.14-pMMP25-Luc and ETV4 wt or ETV4 dn expression plasmids, and the levels of expressed luc activities were measured. C, D, E, B16-BL6 cell-based stable transformants with stable overexpression of MMP25 alone or MMP25 + ETV4 dn were established (see Materials and Methods; Supplementary Figs. S10 and S11). For the established clones, cellular migration (C) and invasion (D) were assessed by the Boyden chamber method and evaluation of cell growth (E) was performed by the MTS assay. Data are means ± SD; N.S: not significant; *P < 0.05, **P < 0.01 and ***P < 0.001. F, Quantitative real-time PCR analysis for the *MMP25* gene was carried out in the indicated cells. The relative expression level in each sample after calibration with the TBP value is shown. G, Double immunofluorescence staining of MMP25 (red) and either S100A8 (green) or S100A9 (green) was performed in the clinically prepared melanoma sections. (Scale, 50 μm). . (For interpretation of the references to color in this figure legend, the reader is referred to the Web version of this article.)

BL6 cells (Supplementary Fig. S3). Random insertions of artificial expression units into chromosomal DNA sometimes induce unexpected alterations in the cell character that occur independently of the functions of the overexpressed target molecules. We therefore carefully selected optimal stable clones that represented each function of the expressed molecules we identified through our previous temporal expression studies. At first, positive clones were selected according to the expression levels of the inserted genes (Supplementary Fig. S3), and then the migration activities of the clones were further checked by an *in vitro* trans-chamber assay (Supplementary Fig. S4). Interestingly, the migration activities of each group showed an almost identical pattern within each stable transformant. MCAM alone, ETV4 wt alone and MCAM + ETV4 wt all tended to increase cellular migration among the clones in each group. GFP stable clones, ETV4 dn alone and MCAM + ETV4 dn all showed lower activity for cellular migration. These results reinforced the conclusions of our earlier temporal expression studies. Finally, we selected one representative clone (control GFP #3, MCAM alone #6, ETV4 wt alone #5, ETV4 dn alone #1, MCAM + ETV4 wt #9, MCAM + ETV4 dn #3) in each group and used them to investigate the metastatic migration abilities *in vitro* before performing the *in vivo* study. The highest activity was observed in clone MCAM + ETV4 wt #9. MCAM #6 and ETV4 wt alone #5 also showed positive reactions, but GFP #3, ETV4 dn #1 and MCAM + ETV4 dn #3 all showed reduced activities (Fig. 5A, left). In contrast to the results for migration (Fig. 5A, left), there were no remarkable differences in growth among the selected clones except for a slight reduction in growth of the ETV4 dn #1 clone (Fig. 5A, right). To control for possible investigator bias based on the clone selection, we examined whether the cellular behavior observed in the selected B16-BL6 clones matched the results in a transient expression system. We found that the observed patterns of migration and growth activities in the selected clones were indeed very similar to those in the transient expression experiments using not only B16-BL6 cells (Fig. S5A) but also WM-266-4 cells (Fig. S5B).

Next, we used these selected clones displaying reliable cellular behaviors to examine the migration activities *in vivo*. We injected the clones into the tail veins of immunocompetent mice and assessed the level of lung metastasis (Fig. 5B and C). The number of lung tumor nodules derived from clone MCAM + ETV4 wt #9 was significantly larger than that derived from control GFP #3 (Fig. 5B). On the other hand, the number and size of metastatic tumor nodules in the MCAM + ETV4 dn #3-injected group were much smaller even with high expression of foreign MCAM in the injected clone (Supplementary Fig. S3) than those in the MCAM + ETV4 wt #9-injected group. These patterns were also reflected in the H&E staining data (Fig. 5C). The results reveal an unusual role of ETV4 in melanoma lung metastasis *in vivo* and show that its function is greatly enhanced by the S100A8/A9 receptor MCAM.

3.5. MMP25, a key molecule for the regulation of melanoma motility and invasiveness, is strongly induced by ETV4 activation through the S100A8/A9-MCAM axis

We next investigated how ETV4 triggers melanoma aggressiveness. Since ETV4 is a transcription factor, it would be expected to regulate numerous genes. To identify the key ETV4-regulated gene(s) that enhance melanoma metastasis, we searched for candidate genes by a bioinformatics technique. Publicly available data for the PC3 prostate cancer cell line, LoVo colon cancer cell line and TRANSFAC prediction database were used for the ETV4-targeted gene promoter. After combining the collected information, 107 overlapped genes appeared (Supplementary Fig. S6A, Supplementary Table S3). Based on previous reports and online results of functional analysis of the 107 genes, we focused on 18 genes as cancer-related genes. However, none of the genes were significantly associated with the activation of ETV4 in the case of melanoma cells, since their expressions were not affected by either ETV4-wt or -dn overexpression in either WM-115 cells (Supplementary Fig. S6B) or WM-266-4 cells (Supplementary Fig. S6C). Faced with this unexpected lack of association between ETV4 and the genes related to melanoma metastasis, we took another approach to metastasis prediction. Because BRAF plays a critical role in the development of melanoma, and TPL2 on the MCAM pathway plays a critical role in melanoma progression, as described above, we decided to investigate the relation between the RAF-MAP3K family (ARAF, BRAF, RAF1) and TPL2 expression [19–21]. Of course, WM-115 and WM-266-4 cells already harbor constitutively active mutBRAF (V600D) [22,23], but a significant increase in the gene expression of the kinases may further enhance melanoma aggressiveness. In addition, we should not rule out the importance of m*atrix metalloproteinases* (MMPs) in cancer metastatic progression. We therefore examined whether these genes are affected by ETV4 at the transcription level in melanoma cells. As shown in Supplementary Figs. S6D and S6E, although the expression of four key kinases was not affected by ETV4, we fortuitously found that only MMP25 was remarkably upregulated by forced expression of ETV4 wt, but not forced expression of ETV4 dn, in both WM-115 and WM-266-4 cells. This was confirmed by repeating the same experiments (Fig. 6A). By a reporter gene assay using the MMP25 promoter, we further found that ETV4 was able to activate the MMP25 promoter with high efficiency (Fig. 6B). This event was also confirmed by the immunohistochemistry, *i.e.*, MMP25 staining was highly positive in malignant melanoma specimens (Supplementary Fig. S7) in which we had detected pronounced elevation of both MCAM and ETV4 in our earlier study (Fig. 3C). These staining patterns were not observed in the normal skin specimens (Supplementary Fig. S7 and Fig. 3C). In addition, in the *in vitro* trans-chamber assay, stable transformants expressing a high level of foreign MMP25 (Supplementary Fig. S8A, schematic of foreign MMP25 expression; Supplementary Figs. S8B and S8F, expression check; Supplementary Figs. S8C and S8G, migration check; Supplementary Figs. S8D and S8H, invasion check; Supplementary Figs. S8E and S8I, growth check) showed remarkably increased capacity for motility (Fig. 6C) and invasiveness (Fig. 6D) even in the absence of extracellular S100A8/A9. These enhanced abilities were not affected by ETV4 dn overexpression (Fig. 6C and D), except for a negligibly small reduction in growth activity (Fig. 6E). These cellular events observed in the selected clones were consistent with the results obtained in the transient overexpression system (Supplementary Fig. S9A, migration check; Supplementary Fig. S9B, invasion check; Supplementary Fig. S9C, growth check). In contrast, cellular migration and invasion activities were markedly reduced by the treatment with Mmp25 siRNAs (siMmp25 #2 and #3) (Supplementary Fig. S10A, expression check; Supplementary Fig. S10B, migration check; Supplementary Fig. S10C, invasion check). These results suggest that MMP25 plays a critical role in melanoma migration and invasion but not in proliferation. In addition to these *in vitro* results, we further found that Mmp25 siRNA significantly mitigated the metastatic activity of B16-BL6 cells toward the lung in the *in vivo* study on mice (Supplementary Fig. S10D). Finally, we confirmed that overexpression of MMP25 consistently occurred in human melanoma cell lines but not in normal human melanocytes (NMC) in culture (Fig. 6F). In addition, the results of clinical melanoma samples that included normal skin area showed that the melanoma mass and cells that had disseminated into the neighboring keratinocyte layer, where S100A8/A9 (green color) was abundant, were strongly stained with MMP25 (red color) (Fig. 6G).

Collectively, the results suggest an important pathway in melanoma progression. In a melanoma skin lesion, melanoma-stimulated keratinocytes induce S100A8/A9, which binds to melanoma cell surface MCAM, resulting in melanoma metastatic progression through a newly identified pathway, TPL2-ETV4, that is linked to induction of one important candidate for melanoma dissemination, MMP25, and the pathway facilitates the migration of melanoma cells to distant lung tissue (Fig. 7).

4. Discussion

In this study, we reported a novel role of the S100A8/A9-MCAM axis in cancer progression in the primary skin lesions of melanoma cells. We demonstrated that cell surface MCAM functions to activate melanoma dissemination upon binding with extracellular S100A8/A9 secreted from the surrounding skin keratinocytes in the primary cancer area. Analysis of the signaling region downstream of MCAM revealed a novel signaling pathway used by MCAM that plays a crucial role in the migration and invasion of melanoma cells. In brief, binding of S100A8/A9 to MCAM leads to the significant activation of MAP3K TPL2, which in turn induces a much higher level of ETV4 activation, eventually leading to transactivation of MMP25. We found that induction of a remarkable level of MMP25 is a cause of the onset of melanoma dissemination and subsequent distant lung metastasis.

Due to the biological significance of MCAM in the progression of various cancers, many studies have been conducted on the roles of this molecule in cancer, but the relation between the intracellular pathway of MCAM and the signal transduction in cancer biology remains controversial [8,24,25]. We therefore tried to identify an MAP3K associated with MCAM, since MAP3Ks are central kinases for triggering a series of MAPK cascades that regulate several cellular events [26,27]. Based on the results of our candidate-interaction assay using a series of MAP3Ks and subsequent cellular motility assay, we identified TPL2 as a key MAP3K for MCAM signaling in cancer invasiveness. TPL2 (MAP3K8) is also called “Cancer Osaka Thyroid (*COT*)” because it was initially cloned as a transforming kinase gene from a human thyroid carcinoma cell line, suggesting that it has a remarkable function both in melanoma and other cancers [28]. In melanoma, it is known that oncogenic mutation occurs at a high frequency (50%–70%) in another MAP3K, BRAF [16–18,22], which we found does not bind to MCAM. Thus, a BRAF inhibitor has been used as a therapeutic agent for melanoma [29], but its clinical use is problematic, since the treatment sometimes causes drug resistance. This may be due to a compensatory function of TPL2. Johannessen et al. showed that TPL2 causes resistance to a BRAF inhibitor through reactivation of MAPK cascades [30]. These results strongly suggest that TPL2 derived from MCAM plays a non-negligible role in melanoma malignancy.

Our results also revealed a critical transcription factor, ETV4, regulated by the MCAM-TPL2 pathway in melanoma after stimulation with S100A8/A9. Accumulating evidence indicates that ETV4 activates melanoma, breast cancer and other types of cancers [31,32]. To determine how ETV4 positively regulates cancer dissemination, we investigated ETV4 target molecules. It has been reported that ETV4 regulates many cancer-related genes by its function as a transcription factor [19,21,33]. However, it seems that the ETV4-based regulation of genes varies greatly depending on the type of cancer. Complex post-translational modifications depending on cell types may govern ETV4 specificity, which can selectively promote cell proliferation, motility and invasion through cancer progression. In our settings using melanoma cells, we found that ETV4 regulates a large increase in MMP25 and that the elevation plays a pivotal role in melanoma dissemination *in vitro*.

MMP25 is a unique membrane-anchored matrix metalloproteinase that is located on the cell surface via a glycosyl-phosphatidyl inositol (GPI) anchor (Supplementary Fig. S8A) [34]. Increased expression of MMP25 has been found in several types of invasive cancer cells, including glioma, colon and prostate cancer cells [35–37]. In addition, when colon cancer cells were transplanted subcutaneously in mice, MMP25 showed a specific distribution at the infiltrative rim of the cancer nugget, suggesting an important role of MMP25 in dissemination onset of cancer cells at the interface region in the cancer primary site [36]. A similar phenomenon was also observed in our melanoma study (Fig. 6G). Collectively, our results support the idea that MMP25 plays an unusual role in the onset of melanoma dissemination in skin.

An interesting finding in this study was that keratinocytes present at the interface of melanoma strongly induced S100A8/A9. Hoshino et al. reported that various *S100* genes are induced simultaneously in normal fibroblasts and Kupffer cells by stimulation with tumor-derived exosomes [38]. Based on their results, we added melanoma exosomes to the culture of keratinocytes. The keratinocytes showed a remarkable ability to induce S100A8/A9 (Supplementary Figs. S11A–S11D). Thus, melanoma-secreted exosomes may play a crucial role in the production and secretion of S100A8/A9 in surrounding keratinocytes, which in turn may induce dissemination of melanoma cells. Further advanced analysis is required to elucidate the molecular mechanism of melanoma progression in response to the cancer microenvironment.

In conclusion, our study demonstrates a critical role of MCAM in melanoma at the primary skin lesion, where the MCAM ligand S100A8/A9 is induced and secreted from melanoma-stimulated keratinocytes. Downstream signaling analysis showed that MCAM promotes activation of ETV4 through recruitment of TPL2, which is linked to a marked increase in MMP25. The identified pathway could play a major role in activation of the spread of melanoma. This novel pathway may be a potential therapeutic target in melanoma.

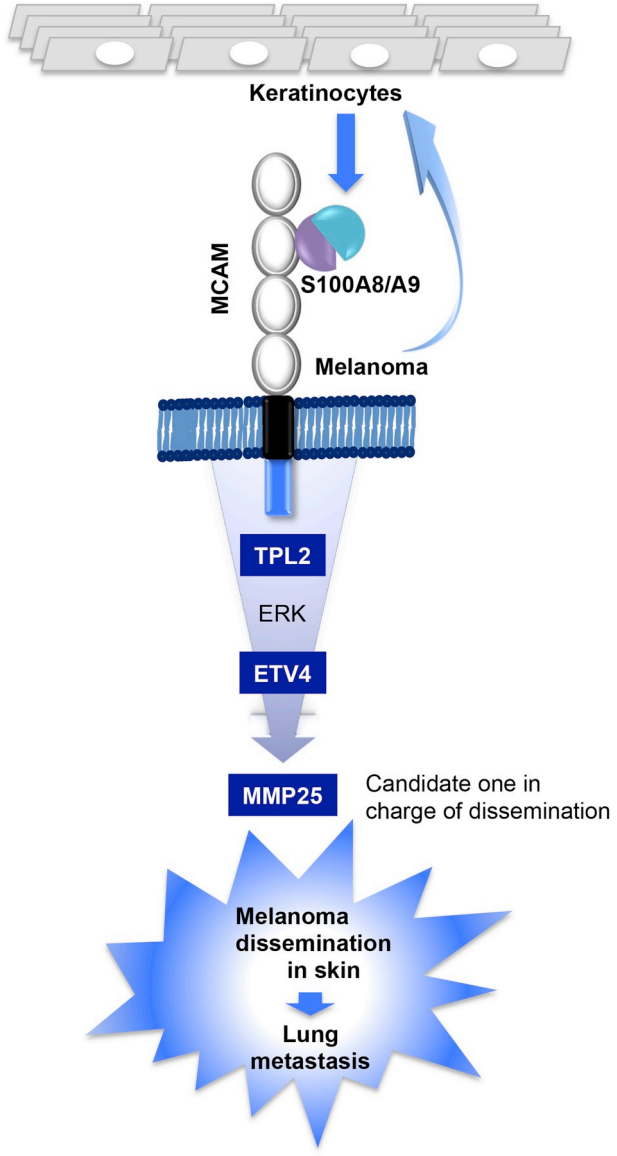

Fig. 7. Schematic of melanoma dissemination in skin in response to S100A8/A9.

Conflicts of interest

The authors declare no conflicts of interest.

Authors' contributions

Conception: M. Sakaguchi.

Design of strategy: Y. Chen, T. Hibino, M. Sakaguchi.

Development of experimental methodology in detail: Y. Chen, M. Sakaguchi.

Key material preparation (plasmids and recombinant proteins): Y. Chen, IW. Sumardika, R. Kinoshita, J. Futami, M. Sakaguchi.

Establishment of key cell sublines: Y. Chen.

Acquisition of key data through studies: Y. Chen.

Acquisition of data from *in vitro* studies: Y. Chen, IW. Sumardika, IM. W. Ruma, R. Kinoshita, E. Kondo, Y. Inoue, A. Yamauchi, H. Murata, K. Yamamoto, S. Tomida, J. Futami, K. Sasai, H. Katayama, M. Kubo, E. W. Putranto, M. Sakaguchi.

Acquisition of data from animal studies: Y. Chen, IW. Sumardika, N. Tomonobu, H. Sato, K. Shien, H. Yamamoto, J. Soh, S. Toyooka.

Key instructive support for animal experiments: M. Liu, B. Sun.

Analysis and interpretation of data: Y. Chen, IW. Sumardika, R. Kinoshita, H. Murata, M. Nishibori, S. Toyooka, M. Sakaguchi.

Writing: Y. Chen, M. Sakaguchi.

Study supervision: M. Sakaguchi.

Acknowledgements

This research was supported in part by funds from the Project for Cancer Research and Therapeutic Evolution (P-CREATE) from the Japan Agency for Medical Research and Development to M.S., by JSPS KAKENHI Grant Number 17H03577 to M.S., and by funds from the Takeda Science Foundation to M.S., the Princess Takamatsu Cancer Research Fund to M.S., the Kobayashi Foundation for Cancer Research to M.S., the Japanese Foundation For Cancer Research to M.S. and the Fujii Memorial Medical Science Foundation to M.S.

Appendix A. Supplementary data

Supplementary data to this article can be found online at https://doi.org/10.1016/j.canlet.2019.03.023.

References

[1] A.L. Jennifer, E.F. David, The melanoma revolution: from UV carcinogenesis to a. new era in therapeutics, Science 346 (2014) 945–949.

[2] N.K. Hayward, J.S. Wilmott, N. Waddell, P.A. Johansson, M.A. Field, K. Nones, A.M. Patch, H. Kakavand, L.B. Alexandrov, H. Burke, V. Jakrot, S. Kazakoff, O. Holmes, C. Leonard, R. Sabarinathan, L. Mularoni, S. Wood, Q. Xu, N. Waddell, V. Tembe, G.M. Pupo, R. De Paoli-Iseppi, R.E. Vilain, P. Shang, L.M.S. Lau, R.A. Dagg, S.J. Schramm, A. Pritchard, K. Dutton-Regester, F. Newell, A. Fitzgerald, C.A. Shang, S.M. Grimmond, H.A. Pickett, J.Y. Yang, J.R. Stretch, A. Behren, R.F. Kefford, P. Hersey, G.V. Long, J. Cebon, M. Shackleton, A.J. Spillane, R.P.M. Saw, N. Lopez-Bigas, J.V. Pearson, J.F. Thompson, R.A. Scolyer, G.J. Mann, Whole-genome landscapes of major melanoma subtypes, Nature 545 (2017) 175–180.

[3] S. Paget, The distribution of secondary growths in cancer of the breast, Cancer Metastasis Rev. 8 (1989) 98–101.

[4] S. Hiratsuka, A. Watanabe, Y. Sakurai, S. Akashi-Takamura, S. Ishibashi, K. Miyake, M. Shibuya, S. Akira, H. Aburatani, Y. Maru, The S100A8-serum amyloid A3-TLR4 paracrine cascade establishes a pre-metastatic phase, Nat. Cell Biol. 10 (2008) 1349–1355.

[5] C. Yin, H. Li, B. Zhang, Y. Liu, G. Lu, S. Lu, L. Sun, Y. Qi, X. Li, W. Chen, RAGE-binding S100A8/A9 promotes. the migration and invasion of human breast cancer cells through actin polymerization and epithelial-mesenchymal transition, Breast Canc. Res. Treat. 142 (2013) 297–309.

[6] T. Hibino, M. Sakaguchi, S. Miyamoto, M. Yamamoto, A. Motoyama, J. Hosoi, T. Shimokata, T. Ito, R. Tsuboi, N.H. Huh, S100A9 is a novel ligand of EMMPRIN that promotes melanoma metastasis, Cancer Res. 73 (2013) 172–183.

[7] M. Sakaguchi, M. Yamamoto, M. Miyai, T. Maeda, J. Hiruma, H. Murata, R. Kinoshita, I.M.W. Ruma, E.W. Putranto, Y. Inoue, S. Morizane, N.H. Huh, R. Tsuboi, T. Hibino, Identification. of an S100A8 receptor neuroplastin-β and its heterodimer formation with EMMPRIN, J. Investig. Dermatol. 136 (2016) 2240–2250.

[8] I.M.W. Ruma, E.W. Putranto, E. Kondo, H. Murata, M. Watanabe, P. Huang, R. Kinoshita, J. Futami, Y. Inoue, A. Yamauchi, I.W. Sumardika, Y.Y. Chen, K. Yamamoto, Y. Nasu, M. Nishibori, T. Hibino, M. Sakaguchi, MCAM, as a. novel receptor for S100A8/A9, mediates progression of malignant melanoma through prominent activation of NF-κB and ROS formation upon ligand binding, Clin. Exp. Metastasis 33 (2016) 609–627.

[9] M. Sakaguchi, M. Watanabe, R. Kinoshita, H. Kaku, H. Ueki, J. Futami, H. Murata, Y. Inoue, S.A. Li, P. Huang, E.W. Putranto, I.M.W. Ruma, Y. Nasu, H. Kumon, N.H. Huh, Dramatic increase in expression of a transgene by insertion of promoters downstream of the cargo gene, Mol. Biotechnol. 56 (2014) 621–630.

[10] I.W. Sumardika, Y.Y. Chen, E. Kondo, Y. Inoue, I.M.W. Ruma, H. Murata, R. Kinoshita, K.I. Yamamoto, S. Tomida, K. Shien, H. Sato, A. Yamauchi, J. Futami, E.W. Putranto, T. Hibino, S. Toyooka, M. Nishibori, M. Sakaguchi, ß-1,3-galactosyl-O-glycosyl-glycoprotein ß-1,6-N- acetylglucosaminyltransferase 3 increases MCAM stability, which enhances S100A8/A9- mediated cancer motility, Oncol. Res. 26 (2017) 431–444.

[11] A. Saltari, F. Truzzi, M. Quadri, R. Lotti, E. Palazzo, G. Grisendi, N. Tiso, A. Marconi, C. Pincelli, CD271 down-regulation promotes melanoma progression and invasion in three-dimensional models and in zebrafish, J. Investig. Dermatol. 136 (2016) 2049–2058.

[12] A.C. Vitari, K.G. Leong, K. Newton, C. Yee, K. O'Rourke, J. Liu, L. Phu, R. Vij, R. Ferrando, S.S. Couto, S. Mohan, A. Pandita, J.A. Hongo, D. Arnott, I.E. Wertz, W.Q. Gao, D.M. French, V.M. Dixit, COP1 is a tumour. suppressor that causes degradation of ETS transcription factors, Nature 474 (2011) 403–406.

[13] S.A. Tomlins, B. Laxman, S.M. Dhanasekaran, B.E. Helgeson, X. Cao, D.S. Morris, A. Menon, X. Jing, Q. Cao, B. Han, J. Yu, L. Wang, J.E. Montie, M.A. Rubin, K.J. Pienta, D. Roulston, R.B. Shah, S. Varambally, R. Mehra, A.M. Chinnaiyan, Distinct classes of chromosomal rearrangements create oncogenic ETS gene fusions in prostate cancer, Nature 448 (2007) 595–599.

[14] F.W. Huang, E. Hodis, M.J. Xu, G.V. Kryukov, L. Chin, L.A. Garraway, Highly recurrent. TERT promoter mutations in human melanoma, Science 339 (2013) 957–959.

[15] C. Slack, N. Alic, A. Foley, M. Cabecinha, M.P. Hoddinott, L. Partridge, The Ras-Erk-ETS- signaling pathway is a drug target for longevity, Cell 162 (2015) 72–83.

[16] H. Davies, G.R. Bignell, C. Cox, P. Stephens, S. Edkins, S. Clegg, J. Teague, H. Woffendin, M.J. Garnett, W. Bottomley, N. Davis, E. Dicks, R. Ewing, Y. Floyd, K. Gray, S. Hall, R. Hawes, J. Hughes, V. Kosmidou, A. Menzies, C. Mould, A. Parker, C. Stevens, S. Watt, S. Hooper, R. Wilson, H. Jayatilake, B.A. Gusterson, C. Cooper, J. Shipley, D. Hargrave, K. Pritchard-Jones, N. Maitland, G. Chenevix-Trench, G.J. Riggins, D.D. Bigner, G. Palmieri, A. Cossu, A. Flanagan, A. Nicholson, J.W. Ho, S.Y. Leung, S.T. Yuen, B.L. Weber, H.F. Seigler, T.L. Darrow, H. Paterson, R. Marais, C.J. Marshall, R. Wooster, M.R. Stratton, P.A. Futreal, Mutations of the. BRAF gene in human cancer, Nature 417 (2002) 949–954.

[17] E. Hodis, I.R. Watson, G.V. Kryukov, S.T. Arold, M. Imielinski, J.P. Theurillat, E. Nickerson, D. Auclair, L. Li, C. Place, D. Dicara, A.H. Ramos, M.S. Lawrence, K. Cibulskis, A. Sivachenko, D. Voet, G. Saksena, N. Stransky, R.C. Onofrio, W. Winckler, K. Ardlie, N. Wagle, J. Wargo, K. Chong, D.L. Morton, K. Stemke-Hale, G. Chen, M. Noble, M. Meyerson, J.E. Ladbury, M.A. Davies, J.E. Gershenwald, S.N. Wagner, D.S. Hoon, D. Schadendorf, E.S. Lander, S.B. Gabriel, G. Getz, L.A. Garraway, L. Chin, A landscape of driver mutations in melanoma, Cell 150 (2012) 251–263.

[18] B. Eskiocak, E.A. McMillan, S. Mendiratta, R.K. Kollipara, H. Zhang, C.G. Humphries, C. Wang, J. Garcia-Rodriguez, M. Ding, A. Zaman, T.I. Rosales, U. Eskiocak, M.P. Smith, J. Sudderth, K. Komurov, R.J. Deberardinis, C. Wellbrock, M.A. Davies, J.A. Wargo, Y. Yu, J.K. De Brabander, N.S. Williams, L. Chin, H. Rizos, G.V. Long, R. Kittler, M.A. White, Biomarker Accessible and chemically Addressable mechanistic subtypes of BRAF melanoma, Cancer Discov. 7 (2017) 832–851.

[19] T.M. Fung, K.Y. Ng, M. Tong, J.N. Chen, S. Chai, K.T. Chan, S. Law, N.P. Lee, M.Y. Choi, B. Li, A.L. Cheung, S.W. Tsao, Y.R. Qin, X.Y. Guan, K.W. Chan, S. Ma, Neuropilin-2 promotes. tumourigenicity and metastasis in oesophageal squamous cell carcinoma through ERK-MAPK-ETV4-MMP-E-cadherin deregulation, J. Pathol. 239 (2016) 309–319.

[20] R. Keld, B. Guo, P. Downey, R. Cummins, C. Gulmann, Y.S. Ang, A.D. Sharrocks, PEA3/ETV4- related transcription factors coupled with active ERK signalling are associated with poor prognosis in gastric adenocarcinoma, Br. J. Canc. 105 (2011) 124–130.

[21] R. Keld, B. Guo, P. Downey, C. Gulmann, Y.S. Ang, A.D. Sharrocks, The ERK MAP kinase- PEA3/ETV4-MMP-1 axis is operative in oesophageal adenocarcinoma, Mol. Canc. 9 (2010) 313.

[22] E.M. Van Allen, N. Wagle, A. Sucker, D.J. Treacy, C.M. Johannessen, E.M. Goetz, C.S. Place, A. Taylor-Weiner, S. Whittaker, G.V. Kryukov, E. Hodis, M. Rosenberg, A. McKenna, K. Cibulskis, D. Farlow, L. Zimmer, U. Hillen, R. Gutzmer, S.M. Goldinger, S. Ugurel, H.J. Gogas, F. Egberts, C. Berking, U. Trefzer, C. Loquai, B. Weide, J.C. Hassel, S.B. Gabriel, S.L. Carter, G. Getz, L.A. Garraway, D. Schadendorf, Dermatologic Cooperative Oncology Group of Germany (DeCOG). The genetic landscape of clinical resistance to RAF inhibition in metastatic melanoma, Cancer Discov. 4 (2014) 94–109.

[23] T. Delgado-Goni, M.F. Miniotis, S. Wantuch, H.G. Parkes, R. Marais, P. Workman, M.O. Leach, M. Beloueche-Babari, The BRAF inhibitor vemurafenib activates mitochondrial metabolism and inhibits hyperpolarized pyruvate-lactate exchange in BRAF-mutant human melanoma cells, Mol. Canc. Therapeut. 15 (2014) 2987–2999.

[24] J.W. Wragg, J.P. Finnity, J.A. Anderson, H.J. Ferguson, E. Porfiri, R.I. Bhatt, P.G. Murray, V.L. Heath, R. Bicknell, MCAM and LAMA4 are highly enriched in tumor blood vessels of renal cell carcinoma and predict patient outcome, Cancer

Res. 76 (2016) 2314–2326.
[25] T. Tu, C. Zhang, H. Yan, Y. Luo, R. Kong, P. Wen, Z. Ye, J. Chen, J. Feng, F. Liu, J.Y. Wu, X. Yan, CD146 acts as a novel receptor for. netrin-1 in promoting angiogenesis and vascular development, Cell Res. 25 (2015) 275–287.
[26] H. Sumimoto, F. Imabayashi, T. Iwata, Y. Kawakami, The BRAF-MAPK signalling. pathway is essential for cancer-immune evasion in human melanoma cells, J. Exp. Med. 203 (2006) 1651–1656.
[27] H.L. Young, E.J. Rowling, M. Bugatti, E. Giurisato, N. Luheshi, I. Arozarena, J.C. Acosta, J. Kamarashev, D.T. Frederick, Z.A. Cooper, A. Reuben, J. Gil, K.T. Flaherty, J.A. Wargo, W. Vermi, M.P. Smith, C. Wellbrock, A. Hurlstone, An adaptive signaling network in melanoma inflammatory niches confers tolerance to MAPK signaling inhibition, J. Exp. Med. 214 (2017) 1691–1710.
[28] J. Miyoshi, T. Higashi, H. Mukai, T. Ohuchi, T. Kakunaga, Structure and transforming potential of the human cot oncogene encoding a putative protein kinase, Mol. Cell Biol. 11 (1991) 4088–4096.
[29] H. Rizos, A.M. Menzies, G.M. Pupo, M.S. Carlino, C. Fung, J. Hyman, L.E. Haydu, B. Mijatov, T.M. Becker, S.C. Boyd, J. Howle, R. Saw, J.F. Thompson, R.F. Kefford, R.A. Scolyer, G.V. Long, BRAF inhibitor resistance mechanisms in metastatic melanoma: spectrum and clinical impact, Clin. Cancer Res. 20 (2014) 1965–1977.
[30] C.M. Johannessen, J.S. Boehm, S.Y. Kim, S.R. Thomas, L. Wardwell, L.A. Johnson, C.M. Emery, N. Stransky, A.P. Cogdill, J. Barretina, G. Caponigro, H. Hieronymus, R.R. Murray, K. Salehi-Ashtiani, D.E. Hill, M. Vidal, J.J. Zhao, X. Yang, O. Alkan, S. Kim, J.L. Harris, C.J. Wilson, V.E. Myer, P.M. Finan, D.E. Root, T.M. Roberts, T. Golub, K.T. Flaherty, R. Dummer, B.L. Weber, W.R. Sellers, R. Schlegel, J.A. Wargo, W.C. Hahn, L.A. Garraway, COT drives resistance to RAF inhibition through MAP kinase pathway reactivation, Nature 468 (2010) 968–972.
[31] L. Hilakivi-Clarke, A. Wärri, K.B. Bouker, X. Zhang, K.L. Cook, L. Jin, A. Zwart, N. Nguyen, R. Hu, M.I. Cruz, S. de Assis, X. Wang, J. Xuan, Y. Wang, B. Wehrenberg, R. Clarke, Effects of in utero exposure to ethinyl estradiol on tamoxifen resistance and breast cancer recurrence in a preclinical model, J. Natl. Cancer Inst. 109 (2016) pii: djw188.
[32] C. Lemaître, J. Tsang, C. Bireau, T. Heidmann, M. Dewannieux, A human endogenous retrovirus-derived gene that can contribute to oncogenesis by activating the ERK pathway and inducing migration and invasion, PLoS Pathog. 13 (2017) e1006451.
[33] R.A. Okimoto, F. Breitenbuecher, V.R. Olivas, W. Wu, B. Gini, M. Hofree, S. Asthana, G. Hrustanovic, J. Flanagan, A. Tulpule, C.M. Blakely, H.J. Haringsma, A.D. Simmons, K. Gowen, J. Suh, V.A. Miller, S. Ali, M. Schuler, T.G. Bivona, Inactivation of Capicua drives cancer metastasis, Nat. Genet. 49 (2017) 87–96.
[34] D. Pei, Leukolysin/MMP25/MT6-MMP: a novel matrix metalloproteinase specifically expressed in the leukocyte lineage, Cell Res. 9 (1999) 291–303.
[35] E. Nuti, F. Casalini, S. Santamaria, P. Gabelloni, S. Bendinelli, E. Da Pozzo, B. Costa, L. Marinelli, V. La Pietra, E. Novellino, M.M. Bernardo, R. Fridman, F. Da Settimo, C. Martini, A. Rossello, Synthesis and biological evaluation in U87MG glioma cells of (ethynylthiophene)sulfonamido-based hydroxamates as matrix metalloproteinase inhibitors, Eur. J. Med. Chem. 46 (2011) 2617–2629.
[36] Q. Sun, C.R. Weber, A. Sohail, M.M. Bernardo, M. Toth, H. Zhao, J.R. Turner, R. Fridman, MMP25 (MT6-MMP) is highly expressed in human colon cancer, promotes tumor growth, and exhibits unique biochemical properties, J. Biol. Chem. 282 (2007) 21998–22010.
[37] A. Sohail, Q. Sun, H. Zhao, M.M. Bernardo, J.A. Cho, R. Fridman, MT4-(MMP17) and MT6-MMP (MMP25), A unique set of membrane-anchored matrix metalloproteinases: properties and expression in cancer, Cancer Metastasis Rev. 27 (2008) 289–302.
[38] A. Hoshino, B. Costa-Silva, T.L. Shen, G. Rodrigues, A. Hashimoto, M. Tesic Mark, H. Molina, S. Kohsaka, A. Di Giannatale, S. Ceder, S. Singh, C. Williams, N. Soplop, K. Uryu, L. Pharmer, T. King, L. Bojmar, A.E. Davies, Y. Ararso, T. Zhang, H. Zhang, J. Hernandez, J.M. Weiss, V.D. Dumont-Cole, K. Kramer, L.H. Wexler, A. Narendran, G.K. Schwartz, J.H. Healey, P. Sandstrom, K.J. Labori, E.H. Kure, P.M. Grandgenett, M.A. Hollingsworth, M. de Sousa, S. Kaur, M. Jain, K. Mallya, S.K. Batra, W.R. Jarnagin, M.S. Brady, O. Fodstad, V. Muller, K. Pantei, A.J. Minn, M.J. Bissell, B.A. Garcia, Y. Kang, V.K. Rajasekhar, C.M. Ghajar, I. Matei, H. Peinado, J. Bromberg, D. Lyden, Tumour exosome integrins determine organotropic metastasis, Nature 527 (2015) 329–335.